OPEN

Myeloid-Epithelial-Reproductive Receptor Tyrosine Kinase and Milk Fat Globule Epidermal Growth Factor 8 Coordinately Improve Remodeling After Myocardial Infarction via Local Delivery of Vascular Endothelial Growth Factor

Kiave-Yune Howangyin, PhD; Ivana Zlatanova, MSc; Cristina Pinto, MSc; Anta Ngkelo, PhD; Clément Cochain, PhD; Marie Rouanet, PhD; José Vilar, PhD; Mathilde Lemitre, BSc; Christian Stockmann, PhD; Bernd K. Fleischmann, MD; Ziad Mallat, MD, PhD; Jean-Sébastien Silvestre, PhD

Background—In infarcted heart, improper clearance of dying cells by activated neighboring phagocytes may precipitate the transition to heart failure. We analyzed the coordinated role of 2 major mediators of efferocytosis, the myeloid-epithelial-reproductive protein tyrosine kinase (Mertk) and the milk fat globule epidermal growth factor (Mfge8), in directing cardiac remodeling by skewing the inflammatory response after myocardial infarction.

Methods and Results—We generated double-deficient mice for Mertk and Mfge8 ($Mertk^{-/-}$/$Mfge8^{-/-}$) and challenged them with acute coronary ligature. Compared with wild-type, Mertk-deficient ($Mertk^{-/-}$), or Mfge8-deficient ($Mfge8^{-/-}$) animals, $Mertk^{-/-}$/$Mfge8^{-/-}$ mice displayed greater alteration in cardiac function and remodeling. Mertk and Mfge8 were expressed mainly by cardiac $Ly6C^{High\ and\ Low}$ monocytes and macrophages. In parallel, $Mertk^{-/-}$/$Mfge8^{-/-}$ bone marrow chimeras manifested increased accumulation of apoptotic cells, enhanced fibrotic area, and larger infarct size, as well as reduced angiogenesis. We found that the abrogation of efferocytosis affected neither the ability of circulating monocytes to infiltrate cardiac tissue nor the number of resident $Ly6C^{High}$ and $Ly6C^{How}$ monocytes/macrophages populating the infarcted milieu. In contrast, combined Mertk and Mfge8 deficiency in $Ly6C^{High}$/$Ly6C^{Low}$ monocytes/macrophages either obtained from in vitro differentiation of bone marrow cells or isolated from infarcted hearts altered their capacity of efferocytosis and subsequently blunted vascular endothelial growth factor A (VEGFA) release. Using $LysMCre^{+}$/$VEGFA^{fl/fl}$ mice, we further identified an important role for myeloid-derived VEGFA in improving cardiac function and angiogenesis.

Conclusions—After myocardial infarction, Mertk- and Mfge8-expressing monocyte/macrophages synergistically engage the clearance of injured cardiomyocytes, favoring the secretion of VEGFA to locally repair the dysfunctional heart. **(*Circulation*. 2016;133:826-839. DOI: 10.1161/CIRCULATIONAHA.115.020857.)**

Key Words: inflammation ■ macrophages ■ myocardial infarction ■ myocarditis ■ neovascularization, physiologic

Improper clearance of dying cells by activated neighboring phagocytes contributes to the establishment and progression of numerous human diseases. As a consequence, efferocytosis-dependent efficient repair is critical to sustain tissue homeostasis by directing the healing of injured tissues through active removal of apoptotic or necrotic cells out of the milieu.[1]

Clinical Perspective on p 839

Cellular necrosis and apoptosis in the acute inflammatory phase of myocardial infarction (MI) are integral components of tissue remodeling and should be dealt with appropriately to improve tissue healing and recovery.[2,3] The externalization of phosphatidylserine on the outer leaflet of the injured cell membrane is one of the earliest signals sufficient to activate the phagocytotic process. The recognition of cells exposing phosphatidylserine is mediated by a few receptors, among

Received August 10, 2015; accepted January 22, 2016.

From INSERM UMRS 970, Université Paris Descartes, Sorbonne Paris Cité, France (K.-Y.H., I.Z., C.P., A.N., M.R., J.V., M.L., C.S., Z.M., J.-S.S.); Institute of Clinical Biochemistry and Pathobiochemistry, University Hospital Würzburg, Germany (C.C.); Institute of Physiology I, Life & Brain Center, University of Bonn, Germany (B.K.F.); and Division of Cardiovascular Medicine, University of Cambridge, Addenbrooke's Hospital, UK (Z.M.).

The online-only Data Supplement is available with this article at http://circ.ahajournals.org/lookup/suppl/doi:10.1161/CIRCULATIONAHA.115.020857/-/DC1.

Correspondence to Jean-Sébastien Silvestre, PhD, PARCC-Inserm U970, Université Paris Descartes, 56 Rue Leblanc, 75015 Paris, France. E-mail jean-sebastien.silvestre@inserm.fr

***Circulation* is available at http://circ.ahajournals.org** **DOI: 10.1161/CIRCULATIONAHA.115.020857**

which myeloid-epithelial-reproductive receptor tyrosine kinase (Mertk) and milk fat globule epidermal growth factor–like factor 8 (Mfge8) are upregulated during inflammation and play nonredundant roles. Mertk receptor on phagocytes recognizes apoptotic cells by bridging Gas6 and protein S, which directly interact with phosphatidylserine.[4,5] Mfge8 is a secretory glycoprotein containing C domains that interact with anionic phospholipids and extracellular matrixes, as well as epidermal growth factor–like domains with an RGD motif that binds integrin $\alpha_v\beta_3$ and $\alpha_v\beta_5$.[6] Thus, Mfge8 appears to be instrumental in cell-cell interactions and has been involved in diverse physiological functions, including fertilization,[7] angiogenesis,[8] atherosclerosis,[9] or innate immunity, through inhibition of inflammasome-induced interleukin (IL)-1β production.[10] One of the prominent functions of Mfge8 is also to link phosphatidylserine of dying cells to integrin $\alpha_v\beta_3$ and $\alpha_v\beta_5$ of phagocytic cells.[11–13] Although the clearance of apoptotic debris by Mertk and Mfge8 has been characterized independently in different pathological settings, whether they also coordinate their functions has not been explored yet. We hypothesized that Mertk and Mfge8 play a critical role in synchronizing efferocytosis within the cardiac tissue after MI and subsequently orchestrate cardiac remodeling.

During the inflammatory reaction, 2 sequential phases defined by the expression of Ly6C on monocytes/macrophages can be identified in the infarcted myocardium.[14,15] The inflammatory Ly-6C^{High} monocyte subset is recruited during the first days after MI, but their number is reduced from day 5 onward, when inflammation resolves in the cardiac wound. Starting at approximately day 3 after MI, the infarct tissue accumulates Ly-6C$^{Int/Low}$ monocytes. The inflammatory Ly-6C^{High} monocyte subset can drive robust inflammation, leading to pathological remodeling, whereas Ly-6C$^{Int/Low}$ monocytes/macrophages seem to promote reparative activities, including angiogenesis.[14,15] However, both monocyte subsets are required for adequate cardiac repair because ablation of each subpopulation is sufficient to disturb the healing process.[14] Many of these monocytes may either die or exit the cardiac tissue, whereas surviving monocytes populating the ischemic milieu may acquire a macrophage phenotype with M1- or M2-like activation mode associated with specific functions in the resolution of inflammation, tissue repair, and remodeling.[16] Recent works also indicate that the adult heart expands distinct populations of macrophages, including monocyte-derived macrophages and subsets of resident macrophages of embryonic origin, with opposite roles in inflammation and cardiac recovery.[17–20]

How different subsets of monocytes/macrophages can govern distinct patterns of cardiac recovery remains largely unknown. Interestingly, efferocytosis can operate a shift in macrophage activation toward M2-like cells.[21] Along this line, dying tumor cells that are cleared through Mertk-dependent efferocytosis robustly induce the transcription of genes encoding wound-healing cytokines, including IL-4, IL-10, IL-13, and transforming growth factor-β (TGFβ).[22]

We reasoned that efficient Mertk- or Mfge8-dependent clearance of dying cardiac cells by tissue monocytes/macrophages dictates their phenotype and is required to fine-tune the reparative process after ischemic cardiac injury. Here, we show that efferocytosis-related signaling commands vascular endothelial growth factor (VEGF) A release by monocytes/macrophages and limits adverse left ventricular remodeling after MI.

Methods

Animals

C57Bl/6J Rj (wild-type [WT]; Janvier Labs, St. Berthevin, France), Mertk$^{-/-}$, Mfge8$^{-/-}$, and Mertk$^{-/-}$/Mfge8$^{-/-}$ mice were 8 to 12 weeks old. Mertk$^{-/-}$, Mfge8$^{-/-}$, and Mertk$^{-/-}$/Mfge8$^{-/-}$ mice were on C57Bl/6J background.[8,23] CD45.1 (Ly5.1) C57Bl/6 mice were purchased from Charles River Labs (France). LysMCre^{+}/VEGF$^{fl/fl}$ and LysMCre^{-}/VEGF$^{fl/fl}$ were provided by Dr C. Stockmann.[24] Cardiac α-actin–green fluorescent protein (α-actin–GFP^{+}) mice on C57Bl/6J background were provided by B.K. Fleischmann.[25] All experiments were conducted according to the French veterinary guidelines and the European community for experimental animal use and were approved by the Institut National de la Santé et de la Recherche Médicale.

Myocardial Infarction

Mice were anesthetized with ketamine (100 mg/kg) and xylazine (10 mg/kg) via intraperitoneal injection and then intubated and ventilated with air with a small-animal respirator (Harvard Apparatus, Courtaboeuf, France). The chest wall was shaved, and a thoracotomy was performed in the fourth left intercostal space. The left ventricle was visualized; the pericardium was then removed; and the left anterior descending artery was permanently ligated with a 7-0 monofilament suture (Peters Surgical, Bobigny, France) at the site of its emergence from under the left atrium, as previously described.[26,27] Significant blanching at the ischemic area was considered indicative of successful coronary occlusion. The thoracotomy was closed with four 6-0 monofilament sutures. The endotracheal tube was removed once spontaneous respiration resumed, and animals were placed on a warm pad maintained at 37°C until they were completely awake.

Bone Marrow Transplantation

Bone marrow (BM) cells were obtained by flushing tibiae and femora of donor mice, as described above. WT mice were lethally irradiated with a total dose of 9.5 Gy and were intravenously injected 24 hours later with 1×10^7 total BM cells from WT, Mertk$^{-/-}$, Mfge8$^{-/-}$, Mertk$^{-/-}$/Mfge8$^{-/-}$, LysMCre^{-}/VEGF$^{fl/f}$, or LysMCre^{+}/VEGF$^{fl/fl}$ cells. Mice were then challenged with MI 10 weeks after BM reconstitution.

Echocardiography

The left ventricular function was assessed by transthoracic echocardiography with a VEVO2100 Biomicroscope (Visualsonics). Mice were anesthetized with isoflurane (1.5% in air), shaved with the use of depilatory cream, and placed on a dedicated eating plate in the supine position, allowing monitoring of respiratory frequency and temperature. Parasternal long-axis views of the left ventricle were obtained with a 40-MHz ultrasound probe (MS550D) at a frame rate between 180 and 240 frames per second. Measurements were performed offline with the Advanced Cardio Package of the VEVO2100 software. Endocardium contours were drawn from telesystolic and telediastolic long-axis views; left ventricular end-diastolic and -systolic volumes and ejection fraction were then measured.

Immunohistochemical Analysis

Fourteen days after MI, hearts were perfused with PBS. Left ventricles were mounted in Cryomatrix (Thermo Scientific) and dropped into frozen isopentane. Sections (7 μm) were cut. For evaluation of apoptosis, heart sections were stained with terminal deoxynucleotidyl transferase dUTP nick-end labeling technology kit (Roche Diagnostics, Meylan, France) according to the manufacturer's instructions. Masson trichrome and Red Sirius stainings were

performed to analyze infarct size and collagen content, respectively. Infarct size was expressed as the ratio of endocardial left ventricular scar length to the total endocardial left ventricular length. Collagen content and the number of capillaries were quantified in the border zone of the infarct scar on a Axioimager Carl Zeiss microscope. Collagen content was measured as the ratio of the total area stained by Red Sirius to the total area of the tissue section on the Image J software. Capillaries were stained with TRITC-conjugated Griffonia simplicifolia lectin (Sigma-Aldrich, Evry, France) and cardiomyocyte membranes with FITC-conjugated wheat germ agglutinin lectin (Sigma-Aldrich). Results were expressed as the ratio of capillaries number to cardiomyocytes.

Immunohistochemical VEGFA Staining on Macrophages

Five days after MI, hearts were perfused with PBS. Left ventricles were mounted in Cryomatrix (Thermo Scientific) and dropped into frozen isopentane. Sections (7 μm) were cut. Heart sections were fixed with 4% paraformaldehyde for 10 minutes at room temperature, stained with TRITC-conjugated wheat germ agglutinin lectin for 1 hour at room temperature, washed with PBS, permeabilized with 0.25% Triton X100 in PBS, washed with PBS, blocked for 30 minutes at room temperature in 5% donkey serum in PBS, stained 2 hours at room temperature with anti-VEGFA (Abcam, Cambridge, Great Britain), washed with PBS, stained 1 hour at room temperature with FITC donkey anti-rabbit IgG, washed with PBS, stained overnight with anti-CD68 (AbD Serotec, Bio-Rad, Kidlington, Oxford, UK) at 4°C, washed with PBS, and stained with Cy5 donkey anti-rat IgG for 1 hour at room temperature. Slides were mounted with DAPI and Mowiol. Images were acquired on a Leica SP8 confocal microscope.

Injection of BM Mononuclear Cells

BM cells were obtained by flushing tibiae and femora of donor mice. Low-density BM-derived mononuclear cells were then isolated by density gradient centrifugation with Ficoll (Histopaque-1083, Sigma-Aldrich). BM mononuclear cells from WT, Mertk$^{-/-}$, Mfge8$^{-/-}$, or Mertk$^{-/-}$/Mfge8$^{-/-}$ were injected 24 hours after MI in WT mice.

Cardiac Efferocytosis

To unravel in vivo cardiac efferocytosis, cardiac α-actin–GFP mice with constitutive expression of GFP in cardiomyocytes were lethally irradiated with a total dose of 9.5 Gy and intravenously injected 24 hours later with 1×10^7 total BM cells isolated from WT or double-knockout Mertk$^{-/-}$/Mfge8$^{-/-}$ animals. MI was induced 10 weeks after BM reconstitution. Three days after MI, cardiac mononuclear cells were isolated as described above and stained. Events were acquired on ImageStream (Amnis Corp) and analyzed on Ideas software. The amount of efferocytosis was determined as the percentage of GFP-positive cells among the population of Ly6C$^{High/Low}$ monocytes/macrophages.

Flow Cytometry Analysis

At 1, 3, 5, 7, and 10 days after MI, hearts were perfused with PBS. Left ventricles were harvested; minced with fine scissors; placed into a cocktail of collagenase I (450 U/mL), collagenase XI (125 U/mL), DNase I (60 U U/mL), and hyaluronidase (60 U/mL; Sigma-Aldrich); and shaken at 37°C for 1 hour, as previously described.[27] Cells were then triturated through a nylon mesh (40 μm) and centrifuged (10 minutes, 400*g*, 4°C). Mononuclear cells were purified by density centrifugation with Ficoll (Histopaque-1083, Sigma-Aldrich; 25 minutes, 400*g*, room temperature). The resulting cell suspensions were washed with PBS, and total leukocyte numbers were determined. Cells harvested from the hearts were stained in PBS at 4°C with the following antibodies: efluor450-conjugated anti-CD11b (M1/70, Biolegend), phycoerythrin-conjugated anti-Ly6G (1A8, BD Pharmingen, Le Pont de Claix, France), phycoerythrin-conjugated anti–NK-1.1 (PK 136, BD Pharmingen), alexa488-conjugated anti-F4/80 (AbD Serotec, Bio-Rad, Kidlington), APC-Cy7–conjugated anti-Ly6C (BD Biosciences, Le Pont de Claix, France), Percp-conjugated anti-CD45 (BD Biosciences), PeAlexa700-conjugated anti-CD45.2, and Percp-conjugated anti-CD45.1 (A20, BD Pharmingen). All antibodies were used at a dilution of 1:100. Monocytes were identified as CD11b$^+$F4/80$^-$Ly6G$^-$Ly6C$^{High\ or\ Low}$. Neutrophils were identified as CD11b$^+$Ly6G^{High}F480$^-$Ly6C^{Int}. Macrophages were identified as CD11b$^+$Ly6G$^-$ F480$^+$Ly6C$^{High\ or\ Low}$. The total number of cells was then normalized to heart weight. Events were acquired on an LSR II flow cytometer (BD Biosciences), and results were analyzed on FlowJo (FlowJo LLC, Ashland, OR).

Protein Expression of Chemokines, Cytokines, and Growth Factors in the Cardiac Tissue

At 1, 3, 5, 7, and 10 days after MI, the upper part of the left ventricle was harvested and homogenized in Tris EDTA NaCl buffer (1 mmol/L EDTA, 10 mmol/L Tris-HCl, pH 7.5, 150 mmol/L NaCl, 10 mg/mL NP40 with antiprotease cocktail; Roche Diagnostics, Meylan, France). Protein concentration was assessed by Lowry assay, and sample concentrations were normalized before quantification of proteins. CCL2, CCL7, IL-1β, IL-6, IL-10, IL-12, IL-13, and tumor necrosis factor-α were quantified with Flowcytomix (ebiosciences, Paris, France) according to the manufacturer's instructions. VEGFA and TGFβ were quantified by ELISA (R&D Systems Europe, Lille, France) according to the manufacturer's instructions.

In Vitro Generation of BM-Derived Macrophages

BM cells were flushed from tibias and femora, washed in PBS with 1% FBS, and cultured in macrophage growth medium for 7 days (RPMI 1640 Glutamax, Fisher Scientific, Illkirsh, France) supplemented with 10% heat-inactivated FCS, 15% L929 medium, and 100 U/mL penicillin/streptomycin. Macrophages were then activated for an additional 24 hours with 1 μg/mL lipopolysaccharide (LPS) and 100 U/mL interferon-γ (IFNγ), 10 ng/mL IL-4, or 10 ng/mL IL-10 (R&D Systems Europe). After 24 hours, the medium was removed, and RPMI 1640 Glutamax supplemented with 10% FCS and 100 U/mL penicillin/streptomycin (complete RPMI medium) was added for 24 hours. Supernatants were harvested for ELISA assays, and cells were washed 3 times in cold PBS and resuspended in RNeasy Lysis Buffer (Rneasy Micro Kit, Qiagen, Courtaboeuf, France). RNA was extracted according to the manufacturer's instructions.

In Vivo Phagocytosis Assay

Phagocytosis by inflammatory macrophages was evaluated by injecting 1×10^7 apoptotic thymocytes or PBS alone (control without phagocytosis) 72 hours after the initial peritoneal injection of thioglycolate (3%; BBL Thioglycolate Medium, brewer modified, BD Biosciences). Three hours after injection, 1 mL PBS was injected into the peritoneum and collected. Peritoneal lavage fluid was centrifuged. Supernatants were harvested and frozen before VEGFA quantification. To evaluate the amount of efferocytosis by flow cytometry, cells were collected and stained with the following antibodies: Alexa 488–conjugated anti-CD11b and V450-conjugated anti-Ly6G (BD Biosciences). The amount of efferocytosis by monocytes/macrophages was expressed as arbitrary fluorescence unit.

Statistical Analysis

Results are expressed as mean±SEM. Kruskal-Wallis 1-way ANOVA was used to compare each measure when there were ≥3 independent groups. Comparisons between groups were performed with Dunn multiple-comparisons test when the ANOVA test was statistically significant. A value of $P<0.05$ was considered significant. The Mann–Whitney test was used to compare 2 groups.

Results

Mertk and Mfge8 Coordinately Improve Cardiac Remodeling After MI

To decipher the respective roles of the 2 major phagocytic proteins Mertk and Mfge8 in cardiac homeostasis, we used

mice deficient for Mertk (Mertk$^{-/-}$), Mfge8 (Mfge8$^{-/-}$), or both (Mertk$^{-/-}$/Mfge8$^{-/-}$) and challenged them with coronary artery ligature to induce acute MI. Mice lacking both Mertk and Mfge8 showed a clear defective cardiac phenotype compared with WT mice, with an intermediate phenotype in the single-knockout (Mertk$^{-/-}$ or Mfge8$^{-/-}$) animals (Figure 1). Notably, ejection fraction was smaller whereas left ventricular end-systolic and -diastolic volumes were higher in Mertk$^{-/-}$/Mfge8$^{-/-}$ mice compared with WT animals (Figure 1A). Alteration in cardiac function was associated with adverse left ventricular remodeling. Along this line, infarct size and collagen content were greater by 1.5- and 1.9-fold, respectively, in Mertk$^{-/-}$/Mfge8$^{-/-}$ mice compared with WT animals (Figure 1B). Furthermore, the number of apoptotic cells was 2-fold higher in Mertk$^{-/-}$/Mfge8$^{-/-}$ mice compared with WT animals (P<0.01). The number of capillaries also tended to be lower in Mertk$^{-/-}$/Mfge8$^{-/-}$ animals compared with WT mice (P<0.05, Mann–Whitney U test; Figure 1B).

Together, these data indicate a central cooperative role for Mertk- and Mfge8-dependent signaling in the control of cardiac remodeling and the recovery of heart function after MI.

Myeloid-Derived Mertk and Mfge8 Improve Remodeling After MI

Because professional phagocytes mainly express Mertk and Mgfe8, we first identified the type of inflammatory cells expressing these proteins in the infarcted heart. Using cells sorted by fluorescence-activated cell sorter, we showed that Mertk and Mfge8 mRNA levels were detected mainly in cardiac Ly6C^{High} and Ly6C^{Low} monocytes/macrophages (CD45$^+$/CD11b$^+$/Ly6G$^-$) and in F4/80-positive macrophages (CD45$^+$/CD11b$^+$/Ly6G$^-$/Ly6C$^+$). Low Mertk and Mfge8 expression was also noticed in infiltrated neutrophils (CD45$^+$/CD11b$^+$/Ly6G$^+$). In contrast, T lymphocytes (CD45$^+$/CD3$^+$) did not express these phagocytic proteins (Figure 2A). We next explored the impact of Mertk and Mfge8 in BM-derived cells using lethally irradiated WT mice transplanted with BM isolated from WT, Mertk$^{-/-}$, Mfge8$^{-/-}$, or Mertk$^{-/-}$/Mfge8$^{-/-}$ mice (Figure 2B and 2C) and subjected to acute MI. Fourteen days after the onset of MI, ejection fraction was lower but left ventricular systolic and diastolic volumes were higher in Mertk$^{-/-}$Mfge8$^{-/-}$ BM compared with WT BM (P<0.001; Figure 2B). Reconstitution with BM from Mertk$^{-/-}$ or Mfge8$^{-/-}$ mice resulted in intermediate effects on cardiac remodeling and heart function (Figure 2).

Infarct size, collagen content, and the number of apoptotic cells were 1.6-, 1.4-, and 2.2-fold higher, respectively, in WT mice transplanted with Mertk$^{-/-}$Mfge8$^{-/-}$ BM compared with those receiving WT BM (P<0.001; Figure 2C). In addition, capillary density tended to be lower in Mertk$^{-/-}$Mfge8$^{-/-}$ BM chimeras (P<0.05, Mann–Whitney U test; Figure 2C). Our results were confirmed by a second set of experiments in which WT mice received intravenous injection of 1×10^6 BM isolated from WT, Mertk$^{-/-}$, Mfge8$^{-/-}$, or Mertk$^{-/-}$/Mfge8$^{-/-}$ animals 24 hours after the onset of ischemia (Figure I in the online-only Data Supplement). Together, these results support a crucial role for Mertk and Mfge8 in BM-related effects in the infarcted heart.

We next sought to understand the mechanisms underlying the influence of myeloid-derived Mertk and Mfge8 in cardiac remodeling after MI, focusing on the double-deficiency context.

We first assessed the extent of efferocytosis of dead cardiomyocytes in the infarcted heart using transgenic mice, in which expression of GFP is under control of the cardiac α-actin promoter (α-actin–GFP$^+$).[25] Using ImageStream assays, we observed that the efferocytosis of dying GFP$^+$ cardiomyocytes was significantly lower in the absence of Mertk and Mfge8, as revealed by the marked decrease in the number of cardiac GFP$^+$ Ly6C$^+$ monocytes/macrophages (CD45$^+$/CD11b$^+$/Ly6G$^-$) isolated from lethally irradiated α-actin–GFP$^+$ mice transplanted with Mertk$^{-/-}$/Mfge8$^{-/-}$ BM compared with those transplanted with WT BM 3 days after the onset of MI (Figure 3A).

We then examined whether abrogation of Mertk and Mfge8 signaling might have altered the ability of inflammatory cells to infiltrate the ischemic milieu. To evaluate the number of infiltrating cells, 1×10^7 mononuclear cells isolated from the BM of CD45.2 WT and Mertk$^{-/-}$/Mfge8$^{-/-}$ animals were intravenously injected into WT CD45.1 mice 6 hours after MI. One day after the injection, we found that the numbers of CD45.2 BM mononuclear cells isolated from WT or Mertk$^{-/-}$/Mfge8$^{-/-}$ animals were similar in CD45.1 infarcted hearts (Figure IIA in the online-only Data Supplement). Along this line, the protein levels of 2 major chemokines, Ccl7 and Ccl2, involved in the recruitment of circulating CCR2-positive inflammatory cells,[26,28] were not affected in WT mice lethally irradiated and transplanted with WT or Mertk$^{-/-}$/Mfge8$^{-/-}$ BM (Figure IIB in the online-only Data Supplement). Hence, alteration of the efficiency of efferocytosis was not related to changes in the number of infiltrated circulating inflammatory cells.

We next hypothesized that a reduction in efferocytosis and a subsequent increase in apoptotic cell number may have altered the number of specific subpopulations of inflammatory cells in the myocardium: cardiac neutrophils and cardiac monocytes/macrophages, which are major players in the setting of MI. Using fluorescence-activated cell sorter analysis of cardiac tissue, we demonstrated that the number of neutrophils was unchanged between WT mice lethally irradiated and transplanted with Mertk$^{-/-}$/Mfge8$^{-/-}$ BM and those transplanted with WT BM (Figure 3B). In the mouse, circulating monocytes are phenotypically and functionally heterogeneous and can be separated according to Ly6C expression.[29,30] We showed that the number of cardiac Ly6C^{High} and Ly6C^{Low} monocytes (CD45$^+$/CD11b$^+$/Ly6G$^-$) was similar in WT mice lethally irradiated and transplanted with Mertk$^{-/-}$/Mfge8$^{-/-}$ BM compared with those transplanted with WT BM (Figure 3B). Transient accumulation of Ly6C^{High} monocytes in the infarcted heart gives rise to distinct population of F4/80-expressing macrophages.[31] However, as for the monocytes subsets, the amount of Ly6C^{High} and Ly6C^{Low} macrophages (CD45$^+$/CD11b$^+$/Ly6G$^-$/F4/80$^+$) was not different between the 2 groups of mice regardless of the time point after the induction of MI (Figure 3B). Among macrophages, embryo-derived tissue resident macrophages are crucial to cardiac remodeling.[17–20] Those cells are characterized mainly by F4/80$^+$ CCR2$^-$ staining in contrast to monocyte-derived macrophages, which are characterized mainly by F4/80$^+$ CCR2$^+$. We quantified the number of CCR2$^-$MHCII^{High} and MHCII^{Low} macrophages in hearts from WT mice lethally irradiated and transplanted with Mertk$^{-/-}$/Mfge8$^{-/-}$ BM and those transplanted with WT BM 7 days after MI. First, the number of CCR2$^-$MHCII^{Low} and MHCII^{High} macrophages is 10 times lower than that of

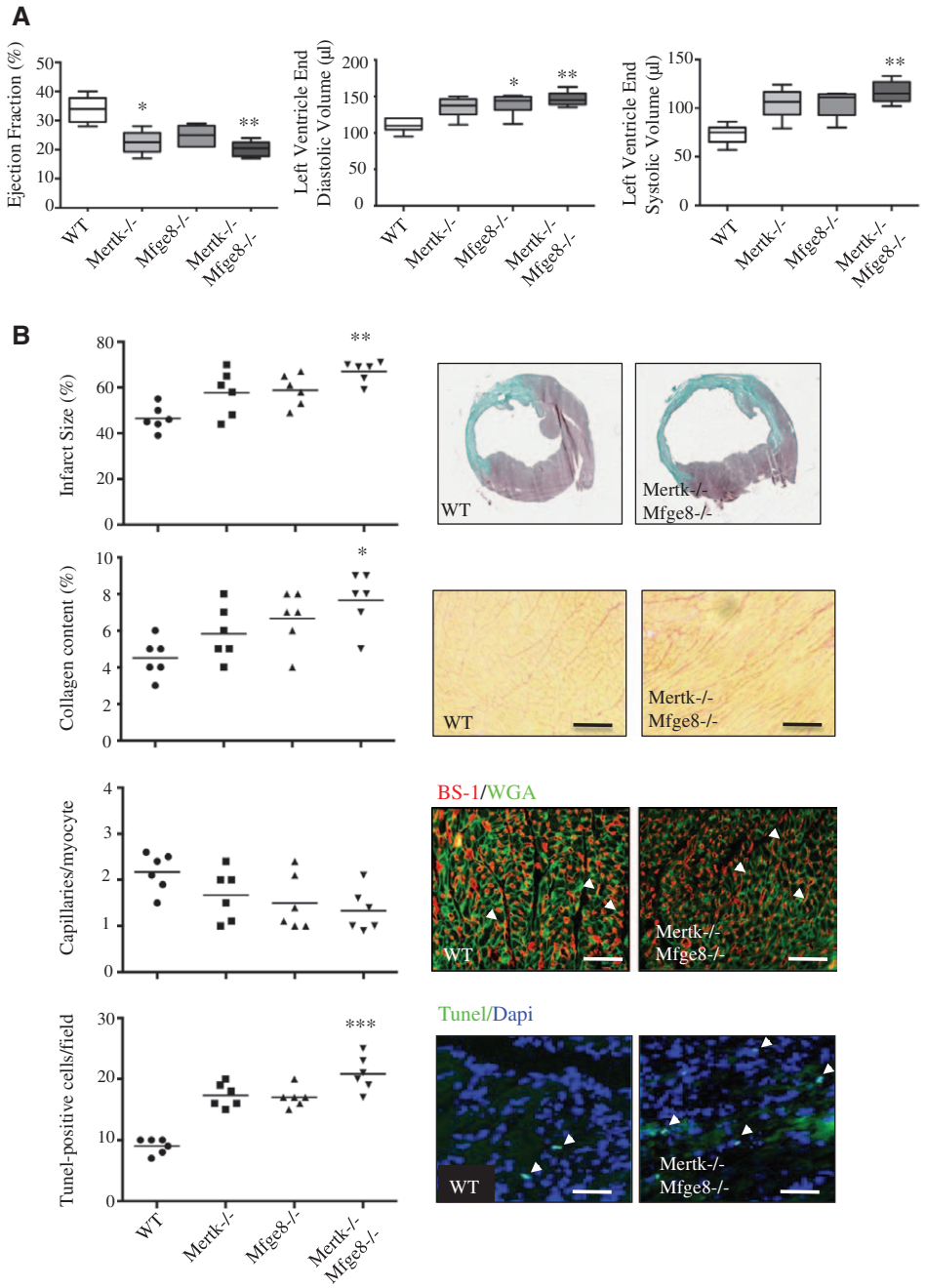

Figure 1. Cardiac healing is impaired in Mertk$^{-/-}$/Mfge8$^{-/-}$ mice. **A**, Echocardiographic analysis 14 days after myocardial infarction. Ejection fraction (%), left ventricular end-diastolic volume (µL), and left ventricular end-systolic volume (µL) are shown for wild-type (WT), Mertk$^{-/-}$, Mfge8$^{-/-}$, and Mertk$^{-/-}$/Mfge8$^{-/-}$ mice. Results are minimum to maximum values. n=6 mice per group. *P<0.05, **P<0.01 vs WT mice (Kruskal-Wallis 1-way ANOVA). **B**, Quantitative analysis of infarct size, collagen content, capillary density, and number of apoptotic cells. Results are presented as scatterplots with mean bar. n=6 mice per group. *P<0.05, **P<0.01 vs WT mice (Kruskal-Wallis 1-way ANOVA). Representative photomicrographs are shown. Arrows point to area of interest. Bar, 100 µm. Mertk indicates myeloid-epithelial-reproductive protein tyrosine kinase; Mfge8, milk fat globule epidermal growth factor; Tunel, terminal deoxynucleotidyl transferase dUTP nick-end labeling; and WGA, wheat germ agglutinin.

CCR2^{+} MHCII cells. Second, the number of CCR2^{-}MHCII^{Low} and MHCII^{High} macrophages was similar in WT mice lethally irradiated and transplanted with Mertk$^{-/-}$/Mfge8$^{-/-}$ BM and those transplanted with WT BM (Figure IIIA in the online-only Data Supplement). Furthermore, to track the origin of macrophages in our experimental conditions, we performed total body irradiation on CD45.1 mice and then transplanted mice with either CD45.2 WT BM or CD45.2 Mertk$^{-/-}$Mfge8$^{-/-}$ BM. After BM reconstitution, we performed MI and assessed CD45.1- and CD45.2-positive macrophages number by flow cytometry. Seven days after MI, <2% of F4/80-positive cells were CD45.1 positive, supporting the statement that the vast majority of cardiac macrophages are not embryo derived in our specific experimental conditions (Figure IIIB in the online-only Data Supplement).

The function of myeloid cells changes over time. Early after the onset of ischemia, the tissue is highly inflammatory, and

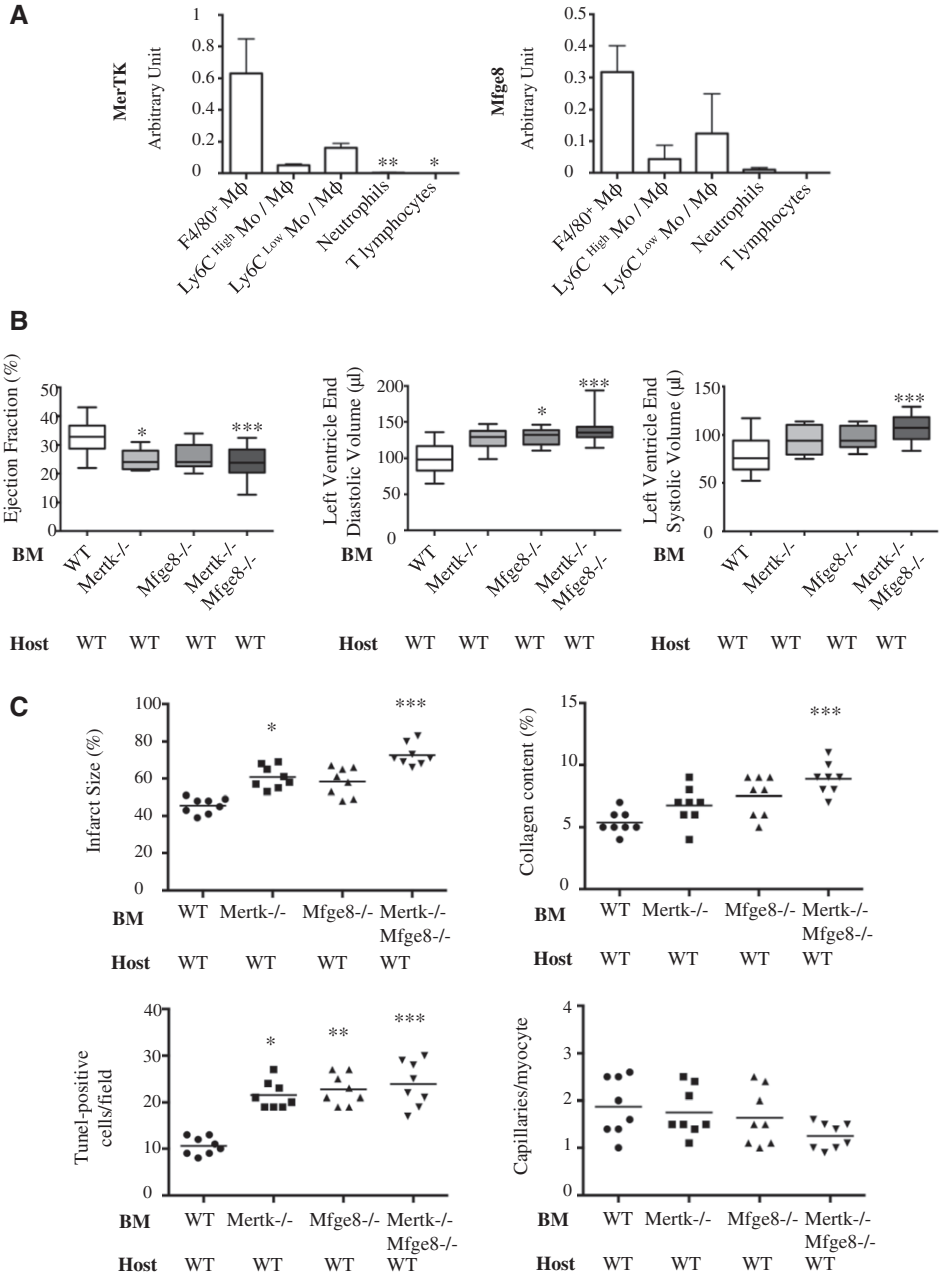

Figure 2. Bone marrow (BM)–derived myeloid-epithelial-reproductive protein tyrosine kinase (Mertk) and milk fat globule epidermal growth factor (Mfge8) improve cardiac remodeling after myocardial infarction (MI). **A**, Mfge8 and Mertk mRNA levels in fluorescence-activated cell sorter–sorted Ly6C^{High} and Ly6C^{Low} monocytes (MO)/macrophages (Mϕ; CD45$^+$CD11b$^+$ Ly6G$^-$ Ly6C$^{High/Low}$), neutrophils (CD45$^+$CD11b$^+$Ly6G$^+$), T lymphocytes (CD45$^+$CD3$^+$), and F4/80-positive macrophages (CD45$^+$/CD11b$^+$/Ly6G$^-$/Ly6C$^+$) isolated from wild-type (WT) mice with MI. Cardiac tissue was harvested at day 1 (neutrophils and T lymphocytes), day 3 (Ly6C^{High} and Ly6C^{Low} monocytes/macrophages), and day 7 (F4/80-positive macrophages) after the onset of MI. Results are mean±SEM. n=3 to 4 mice per group. **B**, Echocardiographic analysis 14 days after MI. Ejection fraction (%), left ventricular end-diastolic volume (µL), and left ventricular end-systolic volume (µL) are shown for lethally irradiated WT mice (Host) transplanted with BM cells isolated from WT, Mertk$^{-/-}$, Mfge8$^{-/-}$, and Mertk$^{-/-}$/Mfge8$^{-/-}$ mice. Results are minimum to maximum values. n=8 to 20 mice per group. *P<0.05, ***P<0.001 vs WT BM chimeras (Kruskal-Wallis 1-way ANOVA). **C**, Quantitative analysis of infarct size (**top left**), collagen content (**top right**), number of apoptotic cells (**bottom left**), and capillary density (**bottom right**). Results are presented as scatterplots with mean bar. n=8 mice per group. *P<0.05, **P<0.01, ***P<0.001 vs WT BM chimeras (Kruskal-Wallis 1-way ANOVA).

Ly-6C^{High} monocytes and macrophages in an M1-like activation mode release high amounts of inflammatory cytokines and proteases. During the following rebuilding phase, the inflammatory activity resolves and gives way to Ly-6C$^{Int/Low}$ monocytes/macrophages. These cells may release VEGFA, TGFβ, and IL-10, supporting angiogenesis, collagen production, and inflammation resolution. We therefore evaluated those modulators of cardiac remodeling in our experimental conditions. Protein levels of IL-1β, IL-6, IL-12, IL-13, tumor necrosis factor-α, and TGFβ were unchanged in the cardiac tissue of WT mice lethally irradiated and transplanted with Mertk$^{-/-}$/Mfge8$^{-/-}$ BM compared with those transplanted with WT BM. Interestingly, at day 3

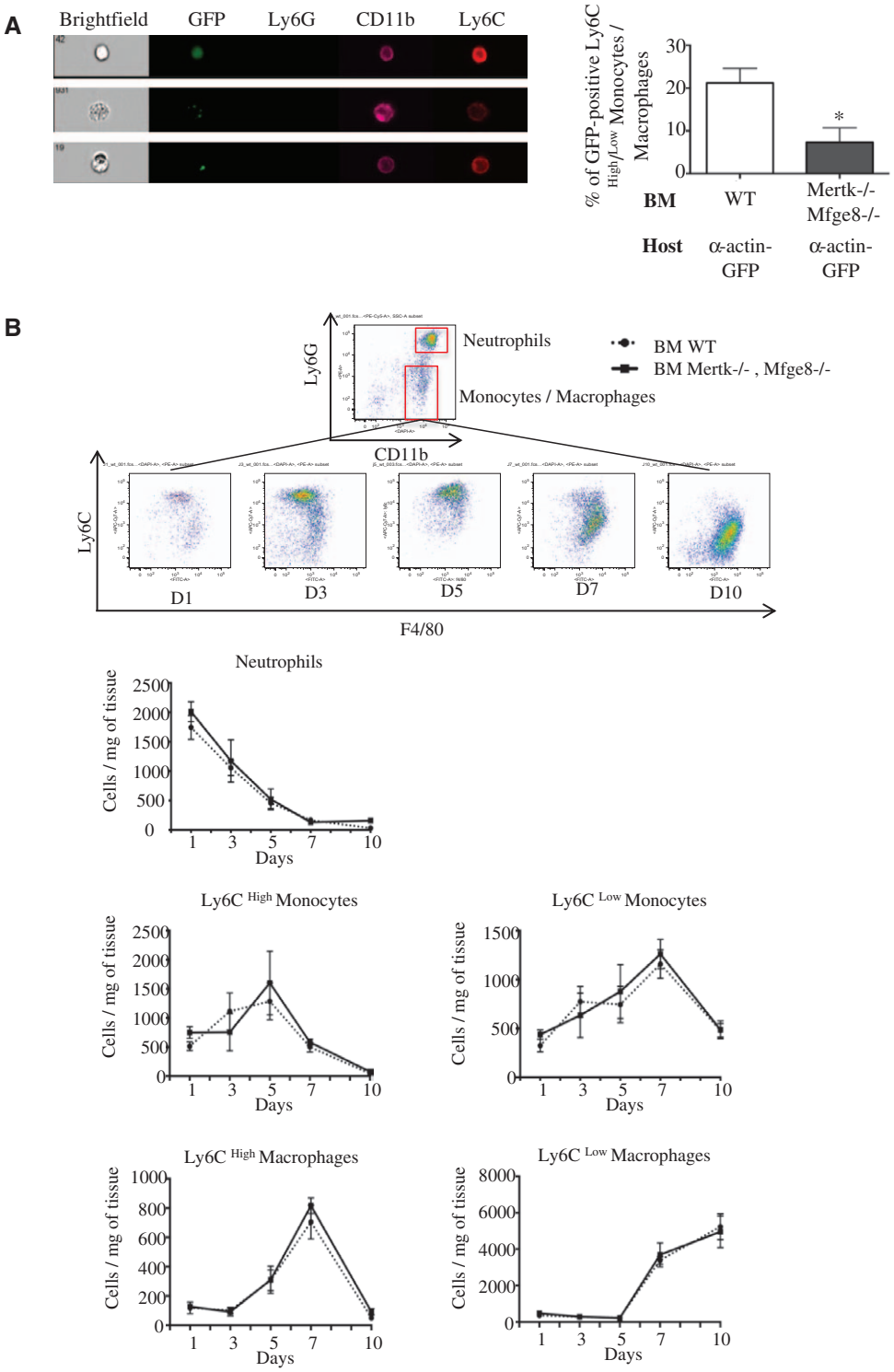

Figure 3. Bone marrow (BM)–derived myeloid-epithelial-reproductive protein tyrosine kinase (Mertk) and milk fat globule epidermal growth factor (Mfge8) do not affect the number of cardiac monocytes/macrophages in the infarcted heart. **A**, Quantification of the number of green fluorescent protein (GFP)–positive Ly6C monocytes/macrophages ($CD45^+CD11b^+Ly6G^-Ly6C^{High/Low}$) by ImageStream analysis in the ischemic heart of α-actin–GFP^+ mice transplanted with wild-type (WT) or $Mertk^{-/-}$/$Mfge8^{-/-}$ BM cells. Representative images of ImageStream assay are shown. Results are mean±SEM. n=4 per group $^{**}P<0.01$ vs WT chimeras (Mann–Whitney test). **B**, Cells harvested from WT mice transplanted with BM cells isolated from WT (BM WT) or $Mertk^{-/-}$/$Mfge8^{-/-}$ (BM $Mertk^{-/-}$/$Mfge8^{-/-}$) mice were analyzed by flow cytometry at days 1, 3, 5, 7, and 10 after myocardial infarction. Results are expressed as the number of cells per 1 mg tissue. Representative examples of neutrophil ($CD11b^+$ $Ly6G^+$), $Ly6C^{High}$ or $Ly6C^{Low}$ monocyte ($CD11b^+Ly6G^-F4/80^-Ly6C^{High\ or\ Low}$), and $Ly6C^{High}$ or $Ly6C^{Low}$ macrophage ($CD11b^+Ly6G^-F4/80^+Ly6C^{High\ or\ Low}$) staining are shown. Results are mean±SEM. n=4 to 5 mice per group (Mann–Whitney test).

after MI, cardiac protein levels of VEGFA (P<0.05) and IL-10 (P=0.0556) were lower in Mertk$^{-/-}$Mfge8$^{-/-}$ BM chimeras compared with controls (Figure 4A).

From these data, we postulated that an alteration in cardiac VEGFA and IL-10 protein levels might be related to a reduction in the ability of cardiac monocytes/macrophages to release these factors. We first showed that CD68-positive cells expressed VEGFA in the infarcted heart (Figure IV in the online-only Data Supplement). We then used fluorescence-activated cell sorter to sort Ly6C^{High} and Ly6C^{Low} monocytes/macrophages from hearts 3 days after infarction. Next, we examined VEGFA and IL-10 expression by quantitative polymerase chain reaction. VEGFA mRNA levels were smaller in sorted Ly6C^{High} and Ly6C^{Low} monocytes/macrophages

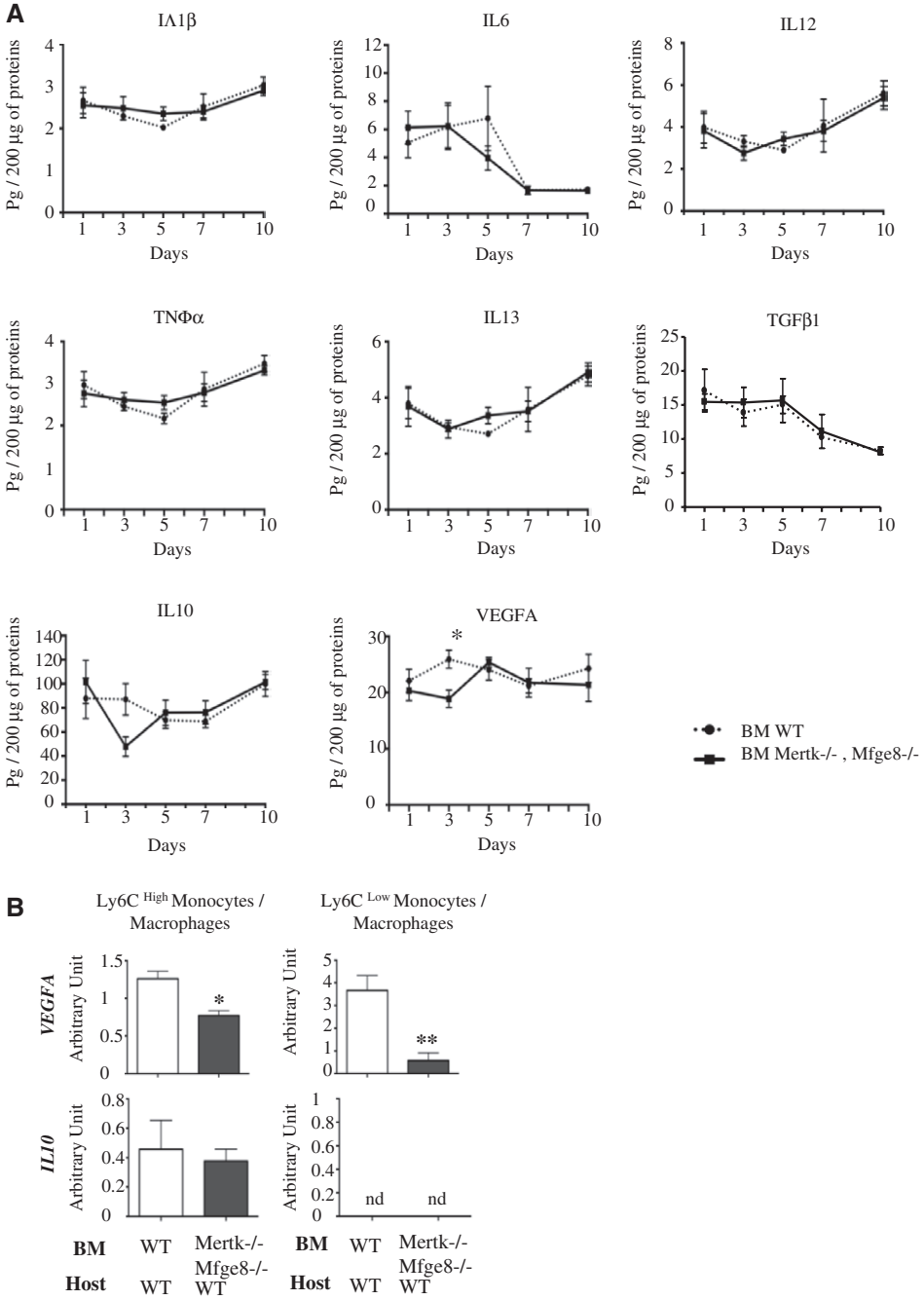

Figure 4. Bone marrow (BM)–derived myeloid-epithelial-reproductive protein tyrosine kinase (Mertk) and milk fat globule epidermal growth factor (Mfge8) govern vascular endothelial growth factor A (VEGFA) release. **A**, Quantitative analysis of cytokines and VEGFA protein levels in the cardiac tissue of lethally irradiated wild-type (WT) mice transplanted with BM-derived cells isolated from WT (BM WT) or Mertk$^{-/-}$/Mfge8$^{-/-}$ (BM Mertk$^{-/-}$/Mfge8$^{-/-}$) animals at days 1, 3, 5, 7, and 10 after myocardial infarction. Results are mean±SEM. n=4 to 5 mice per group. *P<0.05 vs WT BM chimeras at day 3 (Mann–Whitney test). **B**, VEGFA and interleukin (IL)-10 mRNA levels in Ly6C^{High} and Ly6C^{Low} monocytes/macrophages (CD11b^{+}Ly6G^{-}Ly6C$^{High/Low}$) sorted by fluorescence-activated cell sorter from the cardiac tissue of WT mice transplanted with BM from WT or Mertk$^{-/-}$/Mfge8$^{-/-}$ mice at day 3 after myocardial infarction. Results are mean±SEM. n=3 to 4 mice per group. *P<0.05, **P<0.01 vs WT chimeras (Mann–Whitney test). nd indicates not detected; TGFβ, transforming growth factor-β; and TNFα, tumor necrosis factor-α.

collected from WT mice transplanted with Mertk$^{-/-}$Mfge8$^{-/-}$ BM compared with those transplanted with WT BM. No difference was observed in IL-10 mRNA levels (Figure 4B).

In response to various signals, macrophages may balance between the M1- and M2- like modes. We speculated that Mertk/Mgfe8 signaling might modulate macrophage activation state and their ability to release VEGFA. To examine this hypothesis, macrophages were differentiated in vitro from cultured BM isolated from WT or Mertk$^{-/-}$/Mfge8$^{-/-}$ animals and activated with cytokines to trigger various inflammatory profiles. LPS/IFNγ elicited the M1-like mode, whereas IL-4 and IL-10 treatments induced M2-like macrophages.[32] Mfge8 and Mertk were expressed in all types of WT BM–derived macrophages and were not detected in Mertk$^{-/-}$/Mfge8$^{-/-}$ BM–derived macrophages (Figure 5A). Notably, treatment with IL-4 heightened both Mertk and Mfge8 mRNA levels compared with LPS+IFNγ or IL-10 stimulation (Figure 5A). Results also showed that macrophage activation was achieved in these in vitro conditions; that is, mRNAs of the M1 markers (*Cox2* and *NOS2*) were strongly expressed in WT macrophages treated with both LPS and IFNγ, whereas the M2 markers mRNAs (*Ym1*, *Arg1*, *VCAM1*, *RELMα*) were increased in WT macrophages treated with IL-4. Smaller variations were observed among primary cultures for the expression of the M2 marker mRNAs in WT macrophages treated with IL-10 (Figure 5B and 5C). Interestingly, M1 markers were highly expressed in LPS+IFNγ–treated Mertk$^{-/-}$/Mfge8$^{-/-}$ BM–derived macrophages compared with WT (Figure 5B). Conversely, in the setting of IL-4 stimulation, mRNA levels of the M2 markers were downregulated in Mertk$^{-/-}$Mfge8$^{-/-}$ BM–derived macrophages compared with WT cells (Figure 5C). Consistent with this, VEGFA protein release was lower in IL-4– and IL-10–treated Mertk$^{-/-}$Mfge8$^{-/-}$ BM–derived macrophages compared with WT cells (Figure 5D).

Finally, we assessed the putative causal link between Mertk/Mfge8-dependent efferocytosis and VEGFA release. We injected 1×10^7 R18-labeled apoptotic thymocytes in WT mice lethally irradiated and transplanted with WT BM or Mertk$^{-/-}$/Mfge8$^{-/-}$ BM (Figure V in the online-only Data Supplement). Monocytes/macrophages efficiently took up apoptotic thymocytes in WT mice transplanted with WT BM. Interestingly, efferocytosis was significantly lower in WT mice transplanted with Mertk$^{-/-}$/Mfge8$^{-/-}$ BM (Figure 6A). Concomitantly, apoptotic cells triggered VEGFA release in WT mice transplanted with WT BM but not in WT mice transplanted with Mertk$^{-/-}$/Mfge8$^{-/-}$ BM (Figure 6B). Moreover, we challenged the peritoneal lavage fluid obtained after priming with apoptotic cells for endothelial cell proliferation and

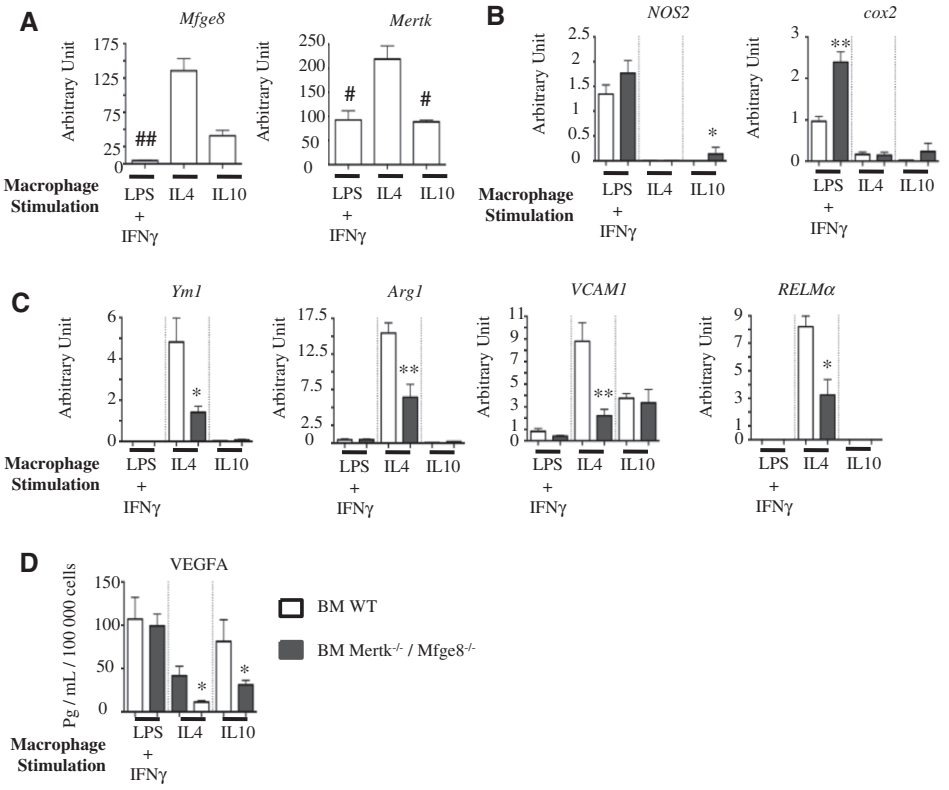

Figure 5. Milk fat globule epidermal growth factor (Mfge8) and myeloid-epithelial-reproductive protein tyrosine kinase (Mertk) control an M2-like activation mode and macrophage-derived vascular endothelial growth factor A (VEGFA) release. cDNA of bone marrow (BM)–differentiated macrophages from wild-type (WT) or Mertk$^{-/-}$/Mfge8$^{-/-}$ mice was analyzed by reverse transcription–quantitative polymerase chain reaction. **A**, Mertk and Mfge8 mRNA levels. Results are mean±SEM. n=4 to 5 mice per group. #P<0.5, ##P<0.001 vs interleukin (IL)-4–treated macrophages (Kruskal-Wallis 1-way ANOVA). **B**, mRNA levels for the markers of the M1-like mode: *NOS2* and *cox2*. Results are mean±SEM. n=4 to 5 mice per group. **C**, mRNA levels for the markers of the M2-like mode: *Ym1*, *Arg1*, *VCAM-1*, and *RELMα*. Results are mean±SEM. n=4 to 5 mice per group. **D**, VEGFA protein levels were quantified in the supernatants of differentiated macrophages by ELISA. Results are mean±SEM. n=4 to 5 mice per group. IFNγ indicates interferon-γ; and LPS, lipopolysaccharide. **B** through **D**: *P<0.05, **P<0.01 vs WT of the same stimulated group of macrophages (Mann–Whitney test).

survival. We found that peritoneal lavage fluid from WT mice transplanted with WT BM protects endothelial cells from apoptosis, in contrast to peritoneal lavage fluid from WT mice transplanted with Mertk$^{-/-}$/Mfge8$^{-/-}$ BM. Concomitantly, peritoneal lavage fluid from WT mice transplanted with Mertk$^{-/-}$/Mfge8$^{-/-}$ BM decreases endothelial cell proliferation compared with peritoneal lavage fluid from WT mice transplanted with WT BM (Figure 6C).

Taken together, these findings identify a role for Mertk- and Mfge8-dependent efferocytosis in promoting an M2 phenotype and in controlling endothelial cell apoptosis and proliferation, at least in part, through the release of VEGFA by macrophages.

Loss of Myeloid Cell–Derived VEGFA Precipitates Adverse Left Ventricular Remodeling After MI

We then hypothesized that loss of myeloid-derived VEGF should recapitulate the effect of Mertk/Mfge8 deficiency on cardiac function and remodeling after MI. We used mice with both alleles of exon 3 of *VEGFA* flanked by loxP sites (VEGF$^{fl/fl}$) crossed onto a background of Cre recombinase expression driven by the lysozyme M promoter (LysMCre^{+}/VEGF$^{fl/fl}$).[33] BM from LysMCre^{+}/VEGF$^{fl/fl}$ mice was then transplanted into lethally irradiated WT animals. We confirmed the selective loss of VEGFA in the BM of LysMCre^{+}/VEGF$^{fl/fl}$ chimeras by quantitative polymerase chain reaction (Figure VIA in the online-only Data Supplement). VEGFA deletion was also established in BM-derived macrophages from these mice polarized toward an M1 or an M2 activation mode (Figure VIB in the online-only Data Supplement). At baseline, no differences in cardiac function, collagen content, and number of capillaries were observed in LysMCre^{+}/VEGF$^{fl/fl}$ chimeras compared with WT chimeras (Figure VIC in the online-only Data Supplement). After the ischemic insult, deletion of VEGF in myeloid cells resulted in lower ejection fraction (P<0.05) and enlarged left ventricular end-systolic volumes (P<0.05) compared with WT mice receiving LysMCre^{-}/VEGFA$^{fl/fl}$ BM (Figure 7A). These effects were associated with superior infarct size and collagen content and a limited number of capillaries in the infarcted hearts of mice reconstituted with VEGF-deficient myeloid cells (Figure 7B).

We highlighted that Mertk/Mfge8–related pathways triggered an M2 activation mode in BM-derived macrophages. We postulated that VEGFA deletion in BM-derived macrophages might mimic this phenotype. To examine this hypothesis, macrophages were differentiated in vitro from cultured BM isolated from LysMCre^{-}/VEGF$^{fl/fl}$ or LysMCre^{+}/VEGF$^{fl/fl}$ animals and activated with LPS+IFNγ, IL-4, or IL-10. M1 markers were strongly expressed in LPS+IFNγ–treated LysMCre^{+}/VEGF$^{fl/fl}$ BM–derived macrophages compared with control (Figure 8A). Conversely, in the setting of IL-4 stimulation, mRNA levels of the M2 markers were downregulated in LysMCre^{+}/VEGF$^{fl/fl}$ BM–derived macrophages compared with control cells (Figure 8B). In addition, we evaluated the phagocytosis capacity of these macrophages in an in vivo efferocytosis assay (Figure 8C). Monocytes/macrophages harvested from peritoneal lavage fluid from WT mice transplanted with LysMCre^{+}/VEGF$^{fl/fl}$ BM and challenged with apoptotic cells showed an

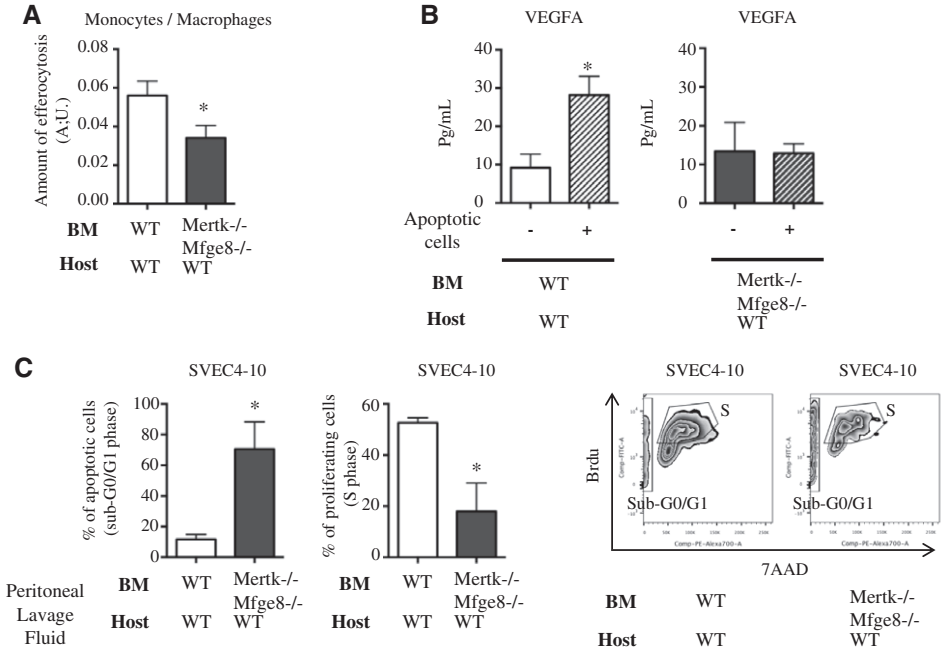

Figure 6. Milk fat globule epidermal growth factor (Mfge8)– and myeloid-epithelial-reproductive protein tyrosine kinase (Mertk)–dependent efferocytosis commands vascular endothelial growth factor A (VEGFA) release and endothelial cell proliferation. Apoptotic thymocytes were injected by intraperitoneal administration in wild-type (WT) mice transplanted with WT or Mertk$^{-/-}$/Mfge8$^{-/-}$ bone marrow (BM). Peritoneal lavage fluid was harvested 3 hours after injection. **A**, Amount of efferocytosis by monocytes/macrophages (CD45^{+}/CD11b^{+}/Ly6G^{-}). Results are mean±SEM. n=4 to 5 mice per group. *P<0.05 vs control. **B**, VEGFA protein levels from the supernatant of peritoneal lavage fluid. Results are mean±SEM. n=4 to 5 mice per group. *P<0.05 vs control. **C**, Supernatants from peritoneal lavage fluid were challenged for endothelial cell proliferation and apoptosis on cultured murine SVEC4-10 endothelial cells. Percentage of sub G0/G1 (apoptotic cells) and S phase (proliferating cells) was assessed with BrdU staining. Representative images of BrdU and 7-Aminoactinomycyn D (7-AAD) staining are shown. Results are mean±SEM. n=4 to 5 mice per group. *P<0.05 vs WT mice transplanted with WT BM (Mann–Whitney test).

amount of efferocytosis similar to that of WT mice transplanted with LysMCre^{-}/VEGF$^{fl/fl}$ BM. In contrast, apoptotic cells did not stimulate VEGFA release in peritoneal lavage fluid harvested from WT mice transplanted with LysMCre^{+}/VEGF$^{fl/fl}$ BM.

Discussion

It is now widely accepted that cardiac remodeling after MI and myeloid cells are intertwined, yet the molecular mechanisms that link monocytes/macrophages to cardiac homeostasis are not well defined. Our results show that efficient Mertk- and Mfge8-dependent clearance of dying cardiac cells by tissue monocytes/macrophages dictates their phenotypes and is critical to the fine-tuning of the reparative process after ischemic cardiac injury. In particular, efferocytosis-related signaling commands VEGFA release by monocytes/macrophages to locally repair the dysfunctional heart.

A number of efferocytosis receptors have been identified in macrophages, suggesting that multiple complementary pathways are involved in the efficient clearance of apoptotic cells. Mertk deficiency alone has already been shown to increase the accumulation of apoptotic cardiomyocytes and compromises systolic performance of the infarcted heart.[34] We provide the first evidence that Mfge8 is also engaged in the recognition of dying cells and in the control of cardiac function and remodeling after MI. Mfge8 is known to link phosphatidylserine of dying cells to integrin $\alpha_v\beta_3$ and $\alpha_v\beta_5$ of phagocytic cells.[11–13] Mfge8 supplementation strongly increases efferocytosis by WT and Mertk-deficient retinal pigment epithelium,[13] implying that Mfge8-related signaling may constitute a nonredundant pathway for the clearance of apoptotic cells. However, coexpression of the active form of Mertk with integrin $\alpha_v\beta_5$ has a synergistic effect on Rac1 activation, lamellipodia formation, and the phagocytosis of apoptotic cells. Gas6 fails to stimulate phagocytosis in β5-deficient cells, suggesting that Mertk is directionally and functionally linked to the Mfge8/integrin pathway to amplify intracellular signals and to internalize apoptotic cells.[35] In addition, whereas Mertk is broadly expressed by all the different macrophage subpopulations, Mfge8 is essential for the phagocytosis of apoptotic cells by inflammation-activated macrophages.[11,36] Although the direct

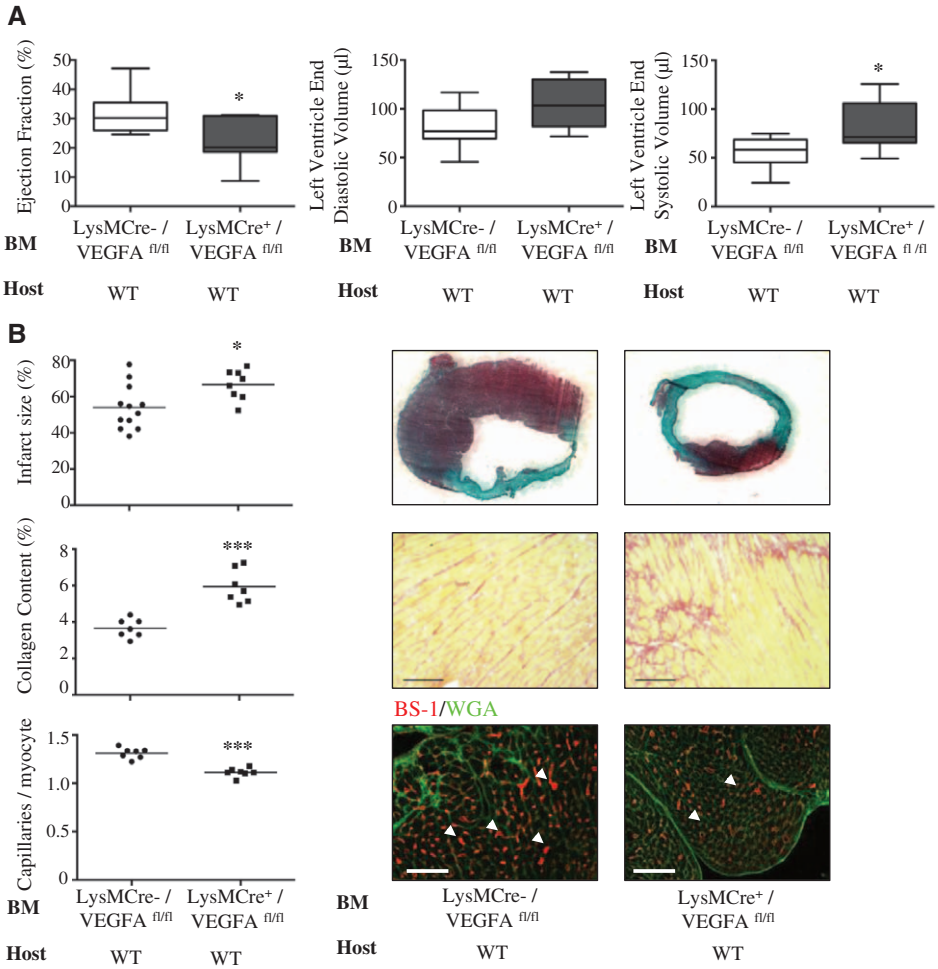

Figure 7. Loss of myeloid cell–derived vascular endothelial growth factor A (VEGFA) precipitates adverse left ventricular remodeling after myocardial infarction (MI). **A**, Echocardiographic analysis 14 days after MI. Ejection fraction (%), left ventricular end-diastolic volume (µL), and left ventricular end-systolic volume (µL) are shown for wild-type (WT) mice (Host) transplanted with bone marrow (BM)–derived cells isolated from LysMCre^{-}VEGF$^{fl/fl}$ or LysMCre^{+}VEGF$^{fl/fl}$ mice. Results are minimum to maximum values. n=7 to 8 mice per group. *P<0.05 vs WT LysMCre^{-}VEGF$^{fl/fl}$ chimeras (Mann–Whitney test). **B**, Quantitative analysis of infarct size, collagen content, number of apoptotic cells, and capillary density. Results are presented as scatterplots with mean bar. n=7 to 12 mice per group. *P<0.05, ***P<0.001 vs WT LysMCre^{-}VEGF$^{fl/fl}$ chimeras (Mann–Whitney test).

or indirect interactions between Mertk and Mfge8 signaling remain to be elucidated, our results clearly indicate that these 2 major phagocytic proteins coordinately participate in tissue homeostasis and recovery from ischemic injury.

Cardiac monocyte and macrophage subsets have been shown to control tissue homeostasis through distinct properties. An inflammatory phenotype (Ly6C^{High} monocytes/M1-type macrophages) initially governs robust inflammation, proteolysis of the extracellular matrix, and clearance of dead cells, a prerequisite for replacing the infarcted milieu with granulation tissue. During the following phase, cells with a lesser inflammatory phenotype (Ly6C$^{Int/Low}$ monocytes/M2-type macrophages) dominate and are thought to release VEGF and TGFβ, supporting angiogenesis and collagen production.[15,17] In our experiments, Mertk and Mfge8 deletion in BM had no effect on the tissue levels of the major chemoattractant molecules, on the recruitment of circulating inflammatory cells, on the accumulation of monocytes, and on the number of circulating monocyte-derived or tissue-resident macrophages within the ischemic myocardium. Hence, the pathophysiological outcome of Mertk and Mfge8 deletion was not related to a defective recruitment or accumulation of inflammatory cells but likely relied on monocyte/macrophage skewing from an inflammatory to a reparative state. In vitro, Mertk and Mfge8 switch macrophages toward an M2-like mode and control the ability of IL-4– or IL-10–treated BM–derived macrophages to release VEGFA. Along this line, we unveiled a role for IL-4 activation in promoting the expression of both Mertk and Mfge8 in cultured BM-derived macrophages, potentially initiating a positive feedback loop to sustain an M2-like phenotype. Mertk- and Mfge8-dependent engulfment of apoptotic cells commands VEGFA release by targeted monocytes/macrophages and shapes endothelial cells proliferation and apoptosis. Therefore, it is tempting to speculate that efficient Mertk- and Mfge8-dependent efferocytosis participates in the transition of cardiac phagocytes from an inflammatory to a VEGFA-related reparative phenotype. However, one cannot refute the hypothesis that Mertk and Mfge8 concomitant loss may affect other protective mediators.

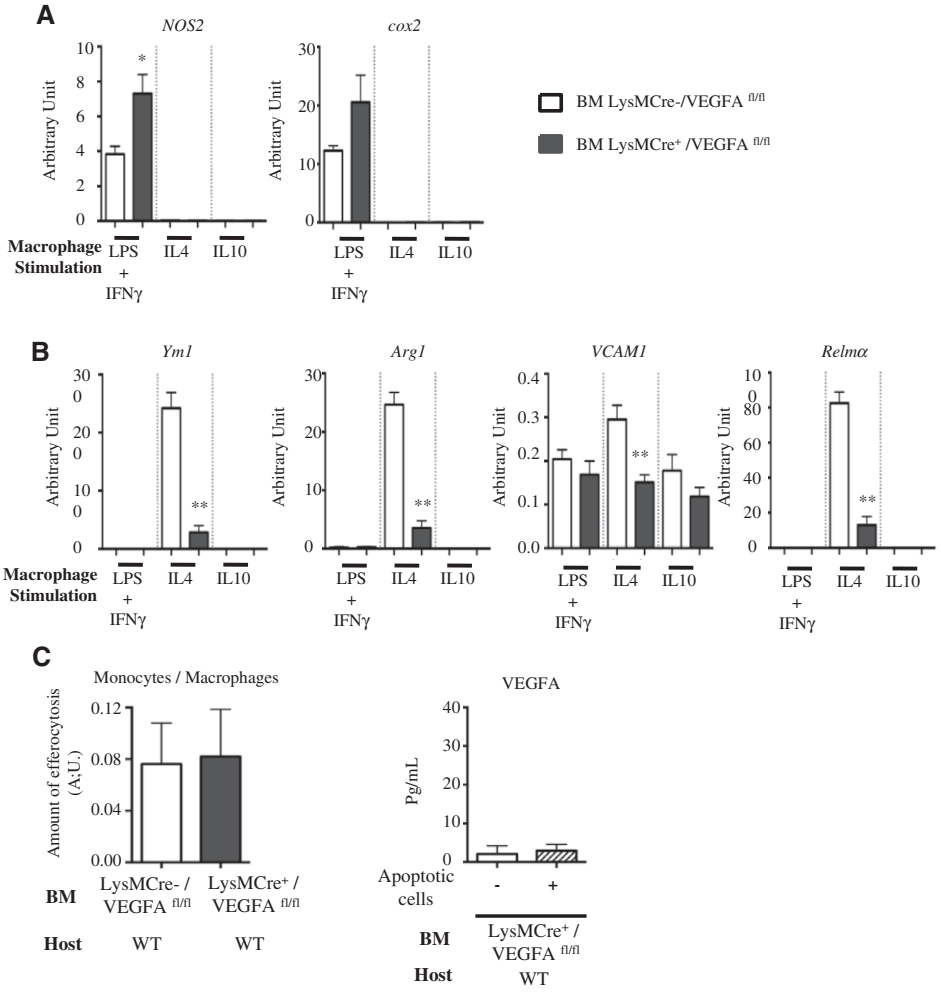

Figure 8. Loss of myeloid cell–derived vascular endothelial growth factor A (VEGFA) activates an M1 phenotype. cDNA from bone marrow (BM)–derived macrophages from LysMCre^{-}VEGF$^{fl/fl}$ and LysMCre^{+}VEGF$^{fl/fl}$ mice were analyzed by reverse transcription–quantitative polymerase chain reaction. **A**, mRNA levels for the markers of the M1-like mode: *NOS2* and *cox2*. **B**, mRNA levels for the markers of the M2-like mode: *Ym1*, *Arg1*, *VCAM-1*, and *RELMα*. Results are mean±SEM. n=4 to 6 mice per group. *P<0.05, **P<0.01 vs LysMCre^{-}VEGF$^{fl/fl}$ of the same stimulated group of macrophages (Mann–Whitney test). **C**, Apoptotic thymocytes were injected in wild-type (WT) mice transplanted with LysMCre^{-}VEGF$^{fl/fl}$ or LysMCre^{+}VEGF$^{fl/fl}$ BM. Peritoneal lavage fluid was harvested 3 hours after injection. **Left**, Amount of efferocytosis by monocytes/macrophages (CD45+/CD11b+/Ly6G-). **Right**, VEGFA protein levels from the supernatant of peritoneal lavage fluid. Results are mean±SEM. n=2 to 3 mice per group. (Mann–Whitney test). IFNγ indicates interferon-γ; IL, interleukin; and LPS, lipopolysaccharide.

Interestingly, we showed that myeloid cell–derived VEGFA plays an essential role in cardiac function and remodeling, likely through activation of the angiogenic process in the border of the infarcted area. Several experimental reports demonstrated the proangiogenic activity of VEGF administration and its associated benefit on cardiac function in different models of MI.[37] However, the net effect of myeloid-derived VEGFA in the reparative process after cardiac ischemic injury was still unexplored. Our results are in line with the role of myeloid-derived VEGF in other disease settings. In a model of pulmonary fibrosis in mice, deletion of VEGFA in myeloid cells reduced the formation of blood vessels and aggravated fibrotic tissue damage.[33] Remarkably, VEGFA also modulates the expression of a major actor of the proteolytic process expressed by endothelial sinusoidal cells and regulates the fibrotic scar in the liver.[38] Hence, myeloid cell–derived VEGF may be a critical regulator of extracellular matrix degradation by cardiac endothelial cells, linking angiogenesis and fibrosis in the cardiac tissue. Consistent with this, we showed that specific ablation of VEGFA in myeloid cells decreased the number of capillaries but raised the collagen content in the infarcted heart. Nonetheless, BM-derived macrophages from LysMCre^{+}/VEGF$^{fl/fl}$ displayed a proinflammatory phenotype, adjoining further complexity to the intrinsic crosstalk between VEGFA and macrophages. Along this line, VEGFA has been shown to induce multiple phenotypic and functional changes in infiltrated Ly6C^{hi} monocytes, endowing them with enhanced proangiogenic and proarteriogenic capabilities.[39]

With respect to translation to the clinics, our results are promising, indicating that the modulation of phagocytic activity by recruited or resident cardiac macrophages may counteract adverse left ventricular remodeling. Notably, the strategy of using autologous apoptotic cells, that is, to improve efferocytosis by reparative phagocytes, has even been clinically tested in patients with chronic heart failure.[40] More interesting, intravenous injection of phosphatidylserine-presenting liposomes is associated with activation of angiogenesis, preservation of small scars, and prevention of ventricular dilatation and remodeling in a rat model of acute MI.[41] Our work suggests that targeting local factors that promote myeloid cell–derived efferocytosis such as the Mertk/Mfge8 axis may counteract the local mediators of inflammation that drive cardiac dysfunction and maladaptation after MI.

Sources of Funding

Dr Silvestre was supported by "Fondation pour la Recherche Médicale" (DEQ20120323734) and "Agence Nationale pour la Recherche (ANR-13-BSV1-0015-01). I. Zlatanova is a recipient of fellowship from CORRDIM-Region île de France.

Disclosures

None.

References

1. Szondy Z, Garabuczi E, Joós G, Tsay GJ, Sarang Z. Impaired clearance of apoptotic cells in chronic inflammatory diseases: therapeutic implications. *Front Immunol*. 2014;5:354. doi: 10.3389/fimmu.2014.00354.
2. Foo RS, Mani K, Kitsis RN. Death begets failure in the heart. *J Clin Invest*. 2005;115:565–571. doi: 10.1172/JCI24569.
3. Whelan RS, Kaplinskiy V, Kitsis RN. Cell death in the pathogenesis of heart disease: mechanisms and significance. *Annu Rev Physiol*. 2010;72:19–44. doi: 10.1146/annurev.physiol.010908.163111.
4. Chen J, Carey K, Godowski PJ. Identification of Gas6 as a ligand for Mer, a neural cell adhesion molecule related receptor tyrosine kinase implicated in cellular transformation. *Oncogene*. 1997;14:2033–2039. doi: 10.1038/sj.onc.1201039.
5. Scott RS, McMahon EJ, Pop SM, Reap EA, Caricchio R, Cohen PL, Earp HS, Matsushima GK. Phagocytosis and clearance of apoptotic cells is mediated by MER. *Nature*. 2001;411:207–211. doi: 10.1038/35075603.
6. Hanayama R, Tanaka M, Miwa K, Shinohara A, Iwamatsu A, Nagata S. Identification of a factor that links apoptotic cells to phagocytes. *Nature*. 2002;417:182–187. doi: 10.1038/417182a.
7. Ensslin MA, Shur BD. Identification of mouse sperm SED1, a bimotif EGF repeat and discoidin-domain protein involved in sperm-egg binding. *Cell*. 2003;114:405–417.
8. Silvestre JS, Théry C, Hamard G, Boddaert J, Aguilar B, Delcayre A, Houbron C, Tamarat R, Blanc-Brude O, Heeneman S, Clergue M, Duriez M, Merval R, Lévy B, Tedgui A, Amigorena S, Mallat Z. Lactadherin promotes VEGF-dependent neovascularization. *Nat Med*. 2005;11:499–506. doi: 10.1038/nm1233.
9. Ait-Oufella H, Kinugawa K, Zoll J, Simon T, Boddaert J, Heeneman S, Blanc-Brude O, Barateau V, Potteaux S, Merval R, Esposito B, Teissier E, Daemen MJ, Lesèche G, Boulanger C, Tedgui A, Mallat Z. Lactadherin deficiency leads to apoptotic cell accumulation and accelerated atherosclerosis in mice. *Circulation*. 2007;115:2168–2177. doi: 10.1161/CIRCULATIONAHA.106.662080.
10. Deroide N, Li X, Lerouet D, Van Vré E, Baker L, Harrison J, Poittevin M, Masters L, Nih L, Margaill I, Iwakura Y, Ryffel B, Pocard M, Tedgui A, Kubis N, Mallat Z. MFGE8 inhibits inflammasome-induced IL-1β production and limits postischemic cerebral injury. *J Clin Invest*. 2013;123:1176–1181. doi: 10.1172/JCI65167.
11. Hanayama R, Tanaka M, Miyasaka K, Aozasa K, Koike M, Uchiyama Y, Nagata S. Autoimmune disease and impaired uptake of apoptotic cells in MFG-E8-deficient mice. *Science*. 2004;304:1147–1150. doi: 10.1126/science.1094359.
12. Kranich J, Krautler NJ, Falsig J, Ballmer B, Li S, Hutter G, Schwarz P, Moos R, Julius C, Miele G, Aguzzi A. Engulfment of cerebral apoptotic bodies controls the course of prion disease in a mouse strain-dependent manner. *J Exp Med*. 2010;207:2271–2281. doi: 10.1084/jem.20092401.
13. Nandrot EF, Anand M, Almeida D, Atabai K, Sheppard D, Finnemann SC. Essential role for MFG-E8 as ligand for alphavbeta5 integrin in diurnal retinal phagocytosis. *Proc Natl Acad Sci U S A*. 2007;104:12005–12010. doi: 10.1073/pnas.0704756104.
14. Nahrendorf M, Swirski FK, Aikawa E, Stangenberg L, Wurdinger T, Figueiredo JL, Libby P, Weissleder R, Pittet MJ. The healing myocardium sequentially mobilizes two monocyte subsets with divergent and complementary functions. *J Exp Med*. 2007;204:3037–3047. doi: 10.1084/jem.20070885.
15. Nahrendorf M, Swirski FK. Monocyte and macrophage heterogeneity in the heart. *Circ Res*. 2013;112:1624–1633. doi: 10.1161/CIRCRESAHA.113.300890.
16. Sica A, Mantovani A. Macrophage plasticity and polarization: in vivo veritas. *J Clin Invest*. 2012;122:787–795. doi: 10.1172/JCI59643.
17. Lavine KJ, Epelman S, Uchida K, Weber KJ, Nichols CG, Schilling JD, Ornitz DM, Randolph GJ, Mann DL. Distinct macrophage lineages contribute to disparate patterns of cardiac recovery and remodeling in the neonatal and adult heart. *Proc Natl Acad Sci USA*. 2014;111:16029–16034. doi: 10.1073/pnas.1406508111.
18. Epelman S, Lavine KJ, Beaudin AE, Sojka DK, Carrero JA, Calderon B, Brija T, Gautier EL, Ivanov S, Satpathy AT, Schilling JD, Schwendener R, Sergin I, Razani B, Forsberg EC, Yokoyama WM, Unanue ER, Colonna M, Randolph GJ, Mann DL. Embryonic and adult-derived resident cardiac macrophages are maintained through distinct mechanisms at steady state and during inflammation. *Immunity*. 2014;40:91–104. doi: 10.1016/j.immuni.2013.11.019.
19. Epelman S, Lavine KJ, Randolph GJ. Origin and functions of tissue macrophages. *Immunity*. 2014;41:21–35. doi: 10.1016/j.immuni.2014.06.013.
20. Heidt T, Courties G, Dutta P, Sager HB, Sebas M, Iwamoto Y, Sun Y, Da Silva N, Panizzi P, van der Laan AM, van der Lahn AM, Swirski FK, Weissleder R, Nahrendorf M. Differential contribution of monocytes to heart macrophages in steady-state and after myocardial infarction. *Circ Res*. 2014;115:284–295. doi: 10.1161/CIRCRESAHA.115.303567.
21. Fadok VA, Bratton DL, Konowal A, Freed PW, Westcott JY, Henson PM. Macrophages that have ingested apoptotic cells in vitro inhibit

proinflammatory cytokine production through autocrine/paracrine mechanisms involving TGF-beta, PGE2, and PAF. *J Clin Invest*. 1998;101:890–898. doi: 10.1172/JCI1112.
22. Stanford JC, Young C, Hicks D, Owens P, Williams A, Vaught DB, Morrison MM, Lim J, Williams M, Brantley-Sieders DM, Balko JM, Tonetti D, Earp HS 3rd, Cook RS. Efferocytosis produces a prometastatic landscape during postpartum mammary gland involution. *J Clin Invest*. 2014;124:4737–4752. doi: 10.1172/JCI76375.
23. Ait-Oufella H, Pouresmail V, Simon T, Blanc-Brude O, Kinugawa K, Merval R, Offenstadt G, Lesèche G, Cohen PL, Tedgui A, Mallat Z. Defective mer receptor tyrosine kinase signaling in bone marrow cells promotes apoptotic cell accumulation and accelerates atherosclerosis. *Arterioscler Thromb Vasc Biol*. 2008;28:1429–1431. doi: 10.1161/ATVBAHA.108.169078.
24. Stockmann C, Doedens A, Weidemann A, Zhang N, Takeda N, Greenberg JI, Cheresh DA, Johnson RS. Deletion of vascular endothelial growth factor in myeloid cells accelerates tumorigenesis. *Nature*. 2008;456:814–818. doi: 10.1038/nature07445.
25. Fleischmann M, Bloch W, Kolossov E, Andressen C, Müller M, Brem G, Hescheler J, Addicks K, Fleischmann BK. Cardiac specific expression of the green fluorescent protein during early murine embryonic development. *FEBS Lett*. 1998;440:370–376.
26. Cochain C, Auvynet C, Poupel L, Vilar J, Dumeau E, Richart A, Récalde A, Zouggari Y, Yin KY, Bruneval P, Renault G, Marchiol C, Bonnin P, Lévy B, Bonecchi R, Locati M, Combadière C, Silvestre JS. The chemokine decoy receptor D6 prevents excessive inflammation and adverse ventricular remodeling after myocardial infarction. *Arterioscler Thromb Vasc Biol*. 2012;32:2206–2213. doi: 10.1161/ATVBAHA.112.254409.
27. Zouggari Y, Ait-Oufella H, Bonnin P, Simon T, Sage AP, Guérin C, Vilar J, Caligiuri G, Tsiantoulas D, Laurans L, Dumeau E, Kotti S, Bruneval P, Charo IF, Binder CJ, Danchin N, Tedgui A, Tedder TF, Silvestre JS, Mallat Z. B lymphocytes trigger monocyte mobilization and impair heart function after acute myocardial infarction. *Nat Med*. 2013;19:1273–1280. doi: 10.1038/nm.3284.
28. Dewald O, Zymek P, Winkelmann K, Koerting A, Ren G, Abou-Khamis T, Michael LH, Rollins BJ, Entman ML, Frangogiannis NG. CCL2/monocyte chemoattractant protein-1 regulates inflammatory responses critical to healing myocardial infarcts. *Circ Res*. 2005;96:881–889. doi: 10.1161/01.RES.0000163017.13772.3a.
29. Geissmann F, Manz MG, Jung S, Sieweke MH, Merad M, Ley K. Development of monocytes, macrophages, and dendritic cells. *Science*. 2010;327:656–661. doi: 10.1126/science.1178331.
30. Carlin LM, Stamatiades EG, Auffray C, Hanna RN, Glover L, Vizcay-Barrena G, Hedrick CC, Cook HT, Diebold S, Geissmann F. Nr4a1-dependent Ly6C(low) monocytes monitor endothelial cells and orchestrate their disposal. *Cell*. 2013;153:362–375. doi: 10.1016/j.cell.2013.03.010.
31. Hilgendorf I, Gerhardt LM, Tan TC, Winter C, Holderried TA, Chousterman BG, Iwamoto Y, Liao R, Zirlik A, Scherer-Crosbie M, Hedrick CC, Libby P, Nahrendorf M, Weissleder R, Swirski FK. Ly-6Chigh monocytes depend on Nr4a1 to balance both inflammatory and reparative phases in the infarcted myocardium. *Circ Res*. 2014;114:1611–1622. doi: 10.1161/CIRCRESAHA.114.303204.
32. Murray PJ, Allen JE, Biswas SK, Fisher EA, Gilroy DW, Goerdt S, Gordon S, Hamilton JA, Ivashkiv LB, Lawrence T, Locati M, Mantovani A, Martinez FO, Mege JL, Mosser DM, Natoli G, Saeij JP, Schultze JL, Shirey KA, Sica A, Suttles J, Udalova I, van Ginderachter JA, Vogel SN, Wynn TA. Macrophage activation and polarization: nomenclature and experimental guidelines. *Immunity*. 2014;41:14–20. doi: 10.1016/j.immuni.2014.06.008.
33. Stockmann C, Kerdiles Y, Nomaksteinsky M, Weidemann A, Takeda N, Doedens A, Torres-Collado AX, Iruela-Arispe L, Nizet V, Johnson RS. Loss of myeloid cell-derived vascular endothelial growth factor accelerates fibrosis. *Proc Natl Acad Sci USA*. 2010;107:4329–4334. doi: 10.1073/pnas.0912766107.
34. Wan E, Yeap XY, Dehn S, Terry R, Novak M, Zhang S, Iwata S, Han X, Homma S, Drosatos K, Lomasney J, Engman DM, Miller SD, Vaughan DE, Morrow JP, Kishore R, Thorp EB. Enhanced efferocytosis of apoptotic cardiomyocytes through myeloid-epithelial-reproductive tyrosine kinase links acute inflammation resolution to cardiac repair after infarction. *Circ Res*. 2013;113:1004–1012. doi: 10.1161/CIRCRESAHA.113.301198.
35. Wu Y, Singh S, Georgescu MM, Birge RB. A role for Mer tyrosine kinase in alphavbeta5 integrin-mediated phagocytosis of apoptotic cells. *J Cell Sci*. 2005;118(pt 3):539–553. doi: 10.1242/jcs.01632.
36. Gautier EL, Shay T, Miller J, Greter M, Jakubzick C, Ivanov S, Helft J, Chow A, Elpek KG, Gordonov S, Mazloom AR, Ma'ayan A, Chua WJ, Hansen TH, Turley SJ, Merad M, Randolph GJ; Immunological Genome Consortium. Gene-expression profiles and transcriptional regulatory pathways that underlie the identity and diversity of mouse tissue macrophages. *Nat Immunol*. 2012;13:1118–1128. doi: 10.1038/ni.2419.
37. Cochain C, Channon KM, Silvestre JS. Angiogenesis in the infarcted myocardium. *Antioxid Redox Signal*. 2013;18:1100–1113. doi: 10.1089/ars.2012.4849.
38. Kantari-Mimoun C, Castells M, Klose R, Meinecke AK, Lemberger UJ, Rautou PE, Pinot-Roussel H, Badoual C, Schrödter K, Österreicher CH, Fandrey J, Stockmann C. Resolution of liver fibrosis requires myeloid cell-driven sinusoidal angiogenesis. *Hepatology*. 2015;61:2042–2055. doi: 10.1002/hep.27635.
39. Avraham-Davidi I, Yona S, Grunewald M, Landsman L, Cochain C, Silvestre JS, Mizrahi H, Faroja M, Strauss-Ayali D, Mack M, Jung S, Keshet E. On-site education of VEGF-recruited monocytes improves their performance as angiogenic and arteriogenic accessory cells. *J Exp Med*. 2013;210:2611–2625. doi: 10.1084/jem.20120690.
40. Torre-Amione G, Anker SD, Bourge RC, Colucci WS, Greenberg BH, Hildebrandt P, Keren A, Motro M, Moyé LA, Otterstad JE, Pratt CM, Ponikowski P, Rouleau JL, Sestier F, Winkelmann BR, Young JB; Advanced Chronic Heart Failure CLinical Assessment of Immune Modulation Therapy Investigators. Results of a non-specific immunomodulation therapy in chronic heart failure (ACCLAIM trial): a placebo-controlled randomised trial. *Lancet*. 2008;371:228–236. doi: 10.1016/S0140-6736(08)60134-8.
41. Harel-Adar T, Ben Mordechai T, Amsalem Y, Feinberg MS, Leor J, Cohen S. Modulation of cardiac macrophages by phosphatidylserine-presenting liposomes improves infarct repair. *Proc Natl Acad Sci USA*. 2011;108:1827–1832. doi: 10.1073/pnas.1015623108.

CLINICAL PERSPECTIVE

Efficient efferocytosis, the process by which apoptotic or necrotic cells are actively removed out of the milieu, is critical to sustain tissue homeostasis by directing the healing of injured tissues. As a consequence, improper clearance of dying cells by activated neighboring phagocytes contributes to the establishment and progression of numerous human diseases. In infarcted heart, alteration of efferocytosis and ineffective elimination of dying cells by galvanized cardiac monocytes/macrophages may precipitate the transition to heart failure. We analyzed the coordinated role of 2 major mediators of efferocytosis, the myeloid-epithelial-reproductive protein tyrosine kinase (Mertk) and the milk fat globule epidermal growth factor (Mfge8), in directing cardiac remodeling by skewing the inflammatory response after myocardial infarction. We showed that Mertk- and Mfge8-expressing monocyte/macrophages synergistically engage the clearance of injured cardiomyocytes, favoring the secretion of the proangiogenic and antifibrotic vascular endothelial growth factor to locally repair the dysfunctional heart. With respect to translation into the clinics, our results are promising, indicating that the modulation of phagocytic activity by recruited or resident cardiac macrophages may counteract adverse left ventricle remodeling. In particular, our work suggests that targeting local factors that promote myeloid cell–derived efferocytosis such as the Mertk/Mfge8 axis may counteract the local mediators of inflammation that drive cardiac dysfunction and maladaptation after myocardial infarction.